Hindawi Publishing Corporation
Journal of Nanotechnology
Volume 2015, Article ID 714072, 7 pages
http://dx.doi.org/10.1155/2015/714072

Research Article

Research on Acetylene Sensing Properties and Mechanism of SnO_2 Based Chemical Gas Sensor Decorated with Sm_2O_3

Qu Zhou,[1] Meiqing Cao,[2] Wude Li,[2] Chao Tang,[1] and Shiping Zhu[1]

[1]*College of Engineering and Technology, Southwest University, Chongqing 400715, China*
[2]*State Grid Chongqing Hechuan District Power Supply Company, Chongqing 401520, China*

Correspondence should be addressed to Qu Zhou; zhouqu@swu.edu.cn

Received 1 July 2015; Revised 25 September 2015; Accepted 29 September 2015

Academic Editor: Zhenyu Li

Acetylene C_2H_2 gas is one of the most important fault characteristic hydrocarbon gases dissolved in oil immersed power transformer oil. This paper reports the successful preparation and characterization of samarium oxide Sm_2O_3 decorated tin oxide SnO_2 based sensors with hierarchical rod structure for C_2H_2 gas detection. Pure and Sm_2O_3 decorated SnO_2 sensing structures were synthesized by a facile hydrothermal method and characterized by XRD, FESEM, TEM, EDS, and XPS measurements, respectively. Planar chemical gas sensors with the synthesis samples were fabricated, and their sensing performances to C_2H_2 gas were systematically performed and automatically recorded by a CGS-1 TP intelligent gas sensing analysis system. The optimum operating temperature of the Sm_2O_3 decorated SnO_2 based sensor towards 50 μL/L of C_2H_2 is 260°C, and its corresponding response value is 38.12, which is 6 times larger than the pure one. Its response time is about 8–10 s and 10–13 s for recovery time. Meanwhile good stability and reproducibility of the decorated sensor to C_2H_2 gas are also obtained. Furthermore, the proposed sensor exhibits excellent C_2H_2 selectivity among some potential interface gases, like H_2 and CO gas. All sensing results indicate the sensor fabricated with oxide Sm_2O_3 decorated SnO_2 nanorods might be a promising candidate for C_2H_2 detection in practice.

1. Introduction

Large-scale power transformers are expensive and significant electric apparatus in electric grid system [1, 2]. At present, a large number of power transformers are still in oil-paper insulation structure, and some insulating defects unavoidably exist during transformer design, manufacturer, installation and operation [3]. Once potential insulating faults happened on power transformers, some fault characteristic gases, like hydrogen, carbon monoxide, carbon dioxide, methane, ethane, ethylene, acetylene, and so forth, would appear and then dissolve into transformer oil [4, 5]. Among them, acetylene gas C_2H_2 is the most effective one to identify thermal and electrical faults. Thus, how to rapidly and accurately detect C_2H_2 gas is currently the subject of intensive research and great attention has been focused on this issue for the past few years [1–6].

In recent years, various types of gas sensing technologies have been proposed to detect transformer fault characteristic gases, such as metal oxide semiconductors [7, 8], gas chromatograph, carbon nanotubes [9], and photoacoustic spectroscopy and Raman spectroscopy [10, 11]. Gas chromatography is mainly used as offline experiment, and spectroscopy is only in the stage of laboratory study and has a long way for practical application. With the advantages of simple manufacture technique, low cost, long life, rapid response, and recovery time, semiconductor SnO_2 may be the most promising sensing technology for detecting and recognizing dissolved fault characteristic gases in transformer oil [12–15]. However, some limitations, like high operating temperature, unsatisfactory selectivity, and poor long-term stability, are still needed to be further improved [16–21]. Doping modification with noble, rare-earth, and transition metals has been proved to be an effective method to improve the sensing properties of metal oxide semiconductors [22–29].

Hence, in this work we proposed the research of semiconductor SnO_2 based chemical gas sensor decorated with rare-earth oxide Sm_2O_3 for C_2H_2 detection. Firstly Sm_2O_3 decorated SnO_2 nanorods were successfully synthesized with a facile and environment friendly hydrothermal method

and characterized by X-ray diffraction (XRD), field emission scanning electron microscopy (FESEM), transmission electron microscopy (TEM), energy dispersive X-ray spectroscopy (EDS), and X-ray photoelectron spectroscopy (XPS) measurements, respectively. And then planar chemical gas sensors with the synthesis samples were fabricated with screen-printing technology, and their sensing performances towards C_2H_2 gas were systematically performed and automatically recorded by a CGS-1 TP intelligent gas sensing analysis system. Finally a possible sensing mechanism was discussed and proposed.

2. Experimental

All the raw chemical reagents were of analytical grade purchased form Chongqing Chuandong Chemical Reagent Co., Ltd. (Chongqing, China), and used as received without any further purification. Sm_2O_3 decorated SnO_2 nanostructures were prepared by a facile and environment friendly hydrothermal method using $Na_2SnO_3{\cdot}3H_2O$, $Sm(NO_3)_3{\cdot}6H_2O$, $C_6H_8O_7{\cdot}H_2O$, NaOH, absolute ethanol, and distilled water as precursors.

In a typical procedure, 0.81 g of $Na_2SnO_3{\cdot}3H_2O$, 0.68 g of NaOH, 30 mL of absolute ethanol, and 30 mL of distilled water were firstly mixed together. Then, 0.05 g of compound metal salt $Sm(NO_3)_3{\cdot}6H_2O$ and 0.24 g of $C_6H_8O_7{\cdot}H_2O$ were added to the mixed solution with intense magnetic stirring. It was magnetically stirred for about 45 min and then transferred into a 100 mL Teflon-lined stainless steel autoclave, sealed and maintained at 180°C for 24 h. After the reaction was completed, the autoclave was cooled to room temperature naturally. The white precipitates were collected and washed with distilled water and absolute ethanol several times to eliminate the unwanted residues. Finally, the products were further air-dried and heated for further use. Pure SnO_2 nanostructures were also prepared for comparison with a similar synthesis route mentioned above.

The crystalline structures of the prepared pure and Sm_2O_3 decorated SnO_2 nanostructures were investigated by X-ray powder diffraction (XRD, Rigaku D/Max-1200X) with Cu Kα radiation (40 kV, 200 mA and λ = 1.5418 Å). The microstructures and morphologies of prepared samples were characterized by means of field emission scanning electron microscope (FESEM, Hillsboro equipped with energy dispersive X-ray (EDS) spectroscopy) and transmission electron micrographs (TEM, Hitachi S-570). Analysis of the X-ray photoelectron spectra (XPS) was performed on an ESCLAB MKII using Al as the exciting source.

Planar chemical gas sensors were fabricated with screen-printing technique, and the ceramic substrates were purchased from Beijing Elite Tech Co., Ltd., China [18]. Figure 1 shows the structure chart of the planar chemical gas sensor. As demonstrated in Figure 1 the planar chemical sensor is composed of three significant components, ceramic substrate, Ag-Pd interdigital electrodes, and sensing materials. The length, width, and height of the planar ceramic substrate are about 13.4, 7, and 1 mm, respectively. The synthesized sensing nanostructures were dispersed with distilled water and absolute ethanol in a weight ratio of 100 : 20 : 10 to form a homogeneous paste. Then the paste was subsequently screen-printed onto the planar ceramic substrate to generate a uniform gas-sensing film. Finally, the fabricated sensor was dried in air at 80°C to volatilize the organic solvent and further aged at 300°C for 2 days to improve its stability before testing.

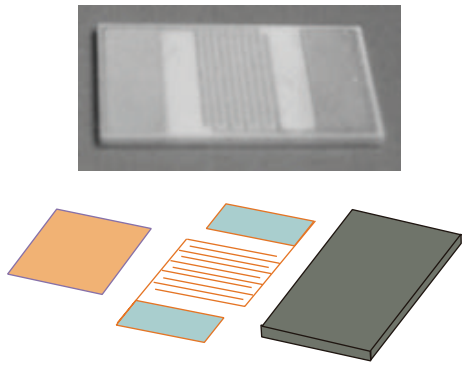

Figure 1: Structure chart of the fabricated planar sensor.

Figure 2: The CGS-1TP gas sensing analysis system.

Gas-sensing properties were measured using the Chemical Gas Sensor-1 Temperature Pressure (CGS-1TP) intelligent gas sensing analysis system [18], which was purchased from Beijing Elite Tech Co., Ltd., China. Figure 2 illustrates the schematic diagram of the CGS-1TP gas sensing analysis system, which could offer an external temperature control ranging from room temperature to 500°C with an adjustment precision of 1°C. The first step in testing process was to put the fabricated gas sensor into the test chamber and fix its electrodes by adjusting the two probes on each side to collect electrical signals. When the sensor resistance reached a constant value, certain amount of C_2H_2 was injected into the chamber by a microinjector through a rubber plug. Open the upper cover of the test chamber to recover the sensor until the resistance attained a new stable value. The sensor resistance and sensitivity were automatically collected and analyzed by the system. And the environmental temperature, relative humidity, and working temperature were also recorded by the analysis system.

The sensor sensitivity (S) in this paper was defined as $S = R_a/R_g$, where R_a represented the resistance of the sensor in air and R_g in certain concentration of C_2H_2 mixed with air,

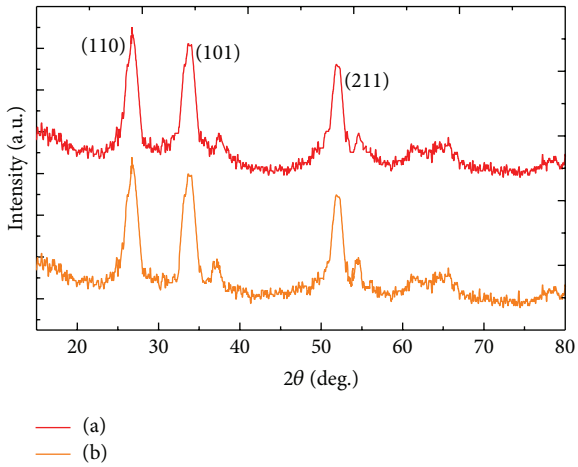

FIGURE 3: Typical XRD patterns of (a) pure and (b) Sm_2O_3 decorated SnO_2 nanostructures.

respectively [30]. The time taken by the sensor to achieve 90% of the total resistance change was designated as the response time in the case of gas adsorption and the recovery time in the case of gas desorption [31]. All gas sensing measurements were repeated several times to ensure the repeatability of the sensor against C_2H_2 gas [31, 32].

3. Results and Discussion

XRD measurement was firstly performed to determine the crystalline structures of the as-synthesized samples. Figure 3 presents the typical XRD patterns of the prepared pure and Sm_2O_3 decorated SnO_2 nanostructures. One can clearly see in Figure 3 that these nanostructures are polycrystalline in nature. The prominent peaks of (110), (101), and (211) and other smaller peaks are well in accordance with the standard spectrum of the tetragonal rutile SnO_2 given in the standard data file (JCPDS file no. 41-1445). No peaks from samarium atom and its oxide are observed, which might be attributed to the high dispersion and the low amount of Sm in the synthesized SnO_2 samples.

To check whether Sm element has been successfully doped into the synthesized SnO_2 nanostructures, energy dispersive X-ray spectroscopy measurement was performed. Figure 4 is the EDS spectrum of the synthesized Sm_2O_3 decorated SnO_2 nanostructures. Peaks from Sn, Sm, and O are observed and the atomic ratio of Sm to Sn is calculated to be about 3.13 at %, which confirms the availability of Sm dopant in the synthesized SnO_2 nanostructures.

To further verify the existence of Sm atom and its valence in the synthesized SnO_2 samples, XPS analyses (Figure 5) were performed and XPS data was collected. Adventitious hydrocarbon C 1s binding energy at 285 eV was used as a reference to correct the energy shift of O 1s. Figure 6 shows the wide survey spectrum of the samples, confirming the existence of Sn, O, and Sm. The binding energies from Sn 3d, 3p, and 3s correspond to Sn^{4+}. And the peak at 1084.3 eV is identified as Sm $2d_{5/2}$, which could be attributed to Sm^{3+} ions.

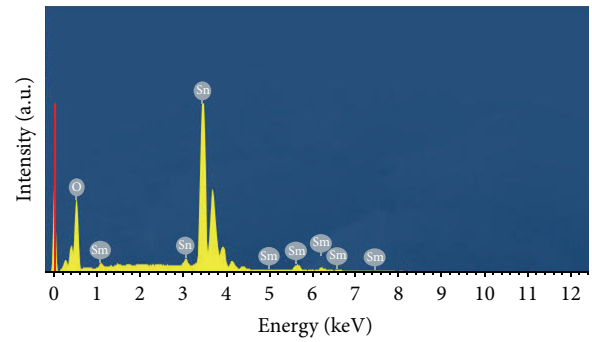

FIGURE 4: EDS spectrum of Sm_2O_3 decorated SnO_2 nanostructures.

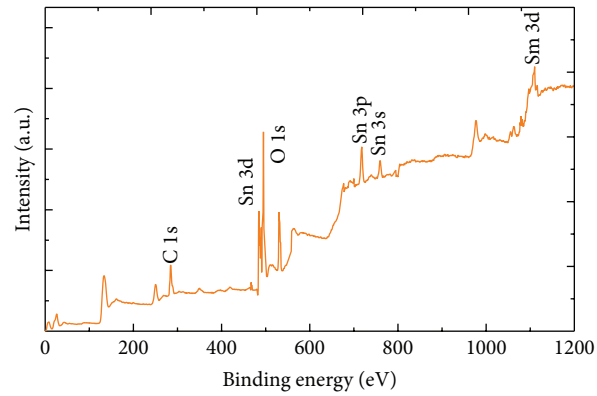

FIGURE 5: XPS survey spectra of Sm_2O_3 decorated SnO_2 nanostructures.

The overall surface morphologies and structural features of the synthesized pure and Sm_2O_3 decorated SnO_2 samples were performed by FESEM, TEM, and SAED measurements and represented in Figure 6. As shown in Figures 6(a)–6(c) numerous rod-like nanostructures with uniform shape and size can be clearly seen, and no other morphologies were observed, revealing a high yield of the products. The TEM image in Figure 6(c) illustrates that both the shape and size of the Sm_2O_3 decorated SnO_2 are exactly consistent with the demonstrated FESEM images. The corresponding SAED pattern as shown in Figure 6(d) verifies the polycrystalline structures of the synthesized Sm_2O_3 decorated SnO_2 nanorods, which coincides well with the XRD results shown in Figure 3.

It is known to all that operating temperature is an important and fundamental characteristic for a semiconductor gas sensor, which has a significant influence on its sensing response. Figure 7 demonstrates the response curves of the prepared pure and Sm_2O_3 decorated SnO_2 nanorods sensors to 50 μL/L of C_2H_2 as a function of working temperature ranging from 140°C to 410°C with an interval of 30°C. Apparently, for each sensor the gas response increases quickly and obtains its maximum and then decreases rapidly with further increase of working temperature. Compared with pure SnO_2 sensor, Sm_2O_3 decorated SnO_2 nanorods sensor exhibits a higher resistance value at the same working temperature. The optimum operating temperature of the decorated one to

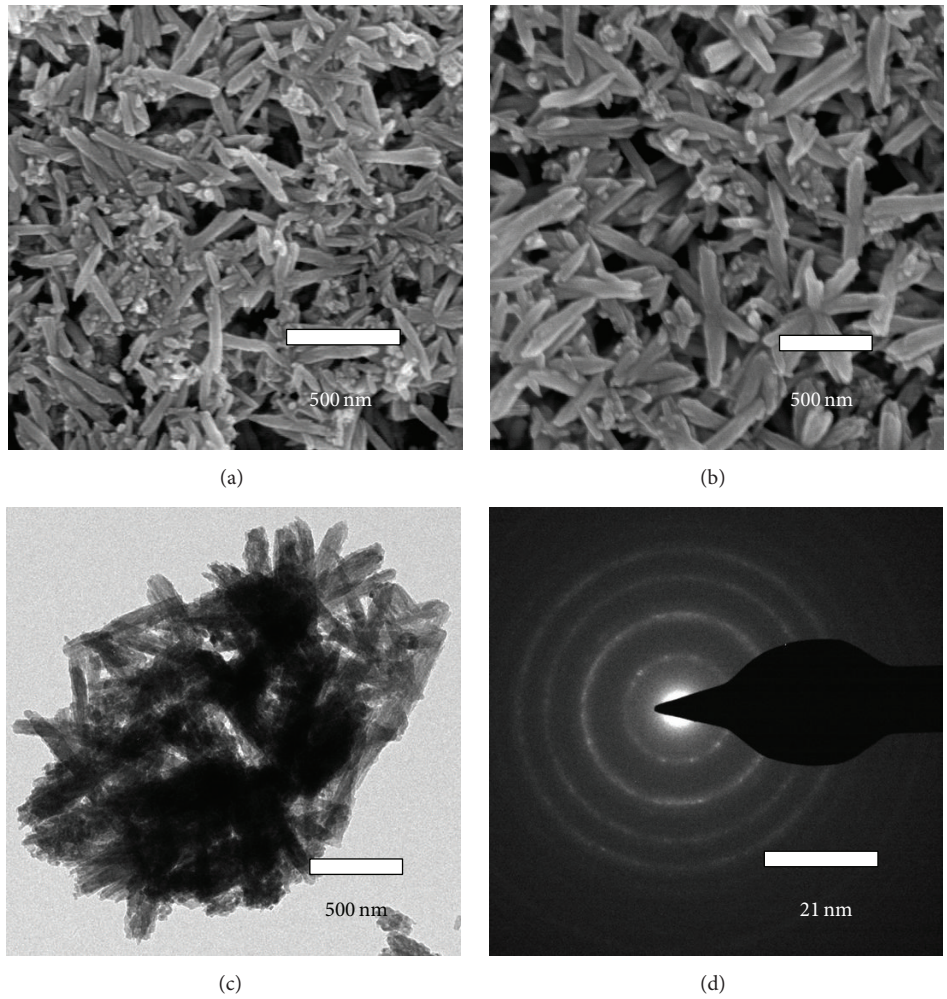

Figure 6: FESEM images of (a) pure SnO_2 and (b) Sm_2O_3 decorated SnO_2 and TEM image (c) and SAED image (d) of Sm_2O_3 decorated SnO_2.

50 μL/L of C_2H_2 is 260°C with the corresponding maximum response value 38.12. And it is 7.53 for the pure one at 320°C, where the sensor exhibits the maximum gas response.

Figure 8 demonstrates the gas responses of the prepared sensors as a function of C_2H_2 concentration with sensor working at its optimum operating temperature measured above. As represented, the sensing responses of the sensors versus C_2H_2 increase greatly with increasing gas concentration in the range of 1–100 μL/L, change much more slowly from 100 μL/L to 400 μL/L, and obtain saturation when exposed to more than 400 μL/L. The saturated sensing responses were measured to be about 68.87 and 18.61 for the Sm_2O_3 decorated SnO_2 nanorods sensor and the pure one.

To investigate the response-recovery characteristic, stability, and repeatability of the Sm_2O_3 decorated SnO_2 nanorods sensor, it was sequentially exposed to various concentrations of C_2H_2 gas as shown in Figure 9 (5, 10, 20, 50, and 100 μL/L) and equal concentration as shown in Figure 10 (20 μL/L). As shown in Figures 9 and 10, the sensor response increases rapidly when exposed to certain concentration of C_2H_2 and decreases dramatically when exposed to air for recovering. The time spent for gas sensing is measured about 8–10 s and 10–13 s for sensor recovering. Meanwhile, the gas response of the sensor always returns to its initial value during the continuous test period, implying a very satisfying reproducibility of the prepared Sm_2O_3 decorated SnO_2 nanorods sensor.

Figure 11 depicts the histogram of the gas responses of the pure and Sm_2O_3 decorated SnO_2 nanorods sensors to 20 μL/L of various gases at 260°C, including C_2H_2, CO, and H_2. It can be clearly seen in Figure 11 that the decorated sensor shows excellent C_2H_2 sensing response among these two potential interface gases.

SnO_2 is a typical n-type oxide semiconducting sensing material, and its gas sensing properties are predominantly controlled by its surface resistance [32–35]. As it is known, when the sensor is exposed to air, oxygen would be absorbed on SnO_2 surface firstly. Due to strong electronegativity, the absorbed oxygen acts as a trap capturing electrons from the condition band of SnO_2 to form chemisorbed oxygen species like O^{2-}, O^-, or O_2^- [36]. Consequently, a depletion region on the surface appears, resulting in a decline of

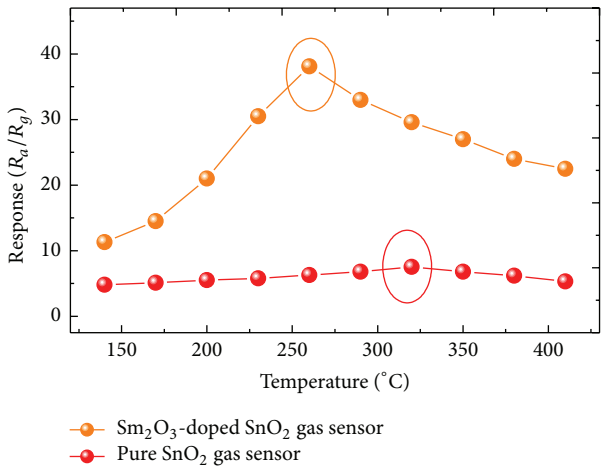

FIGURE 7: Gas responses of the sensors to 50 μL/L of C_2H_2 at various working temperature.

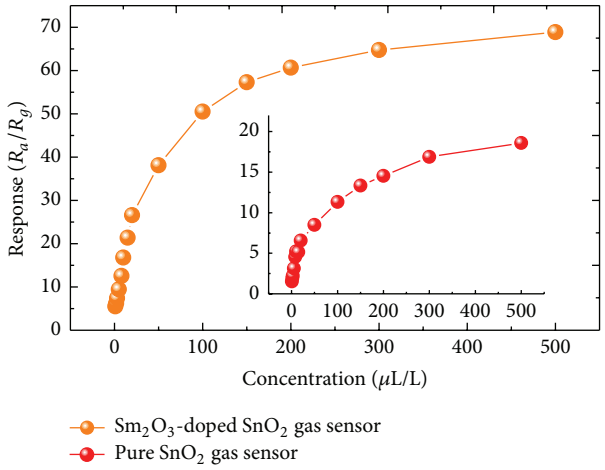

FIGURE 8: Gas responses of the sensors versus different concentration of C_2H_2 from 1 to 500 μL/L.

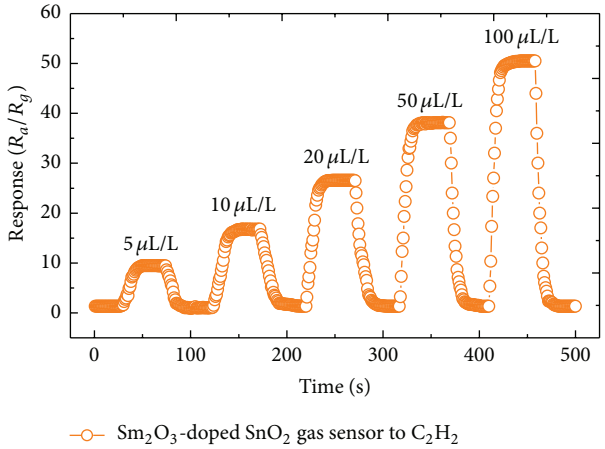

FIGURE 9: Dynamic C_2H_2 sensing transients of the Sm_2O_3 decorated SnO_2 nanorods sensor at 260°C.

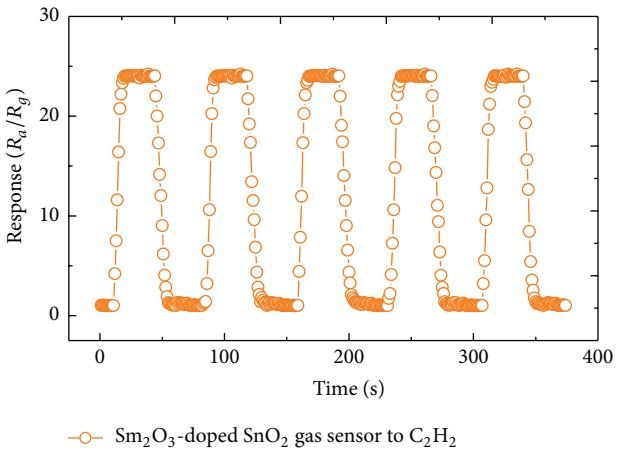

FIGURE 10: Reproducibility of the Sm_2O_3 decorated SnO_2 nanorods sensor to 20 μL/L of C_2H_2 at 260°C.

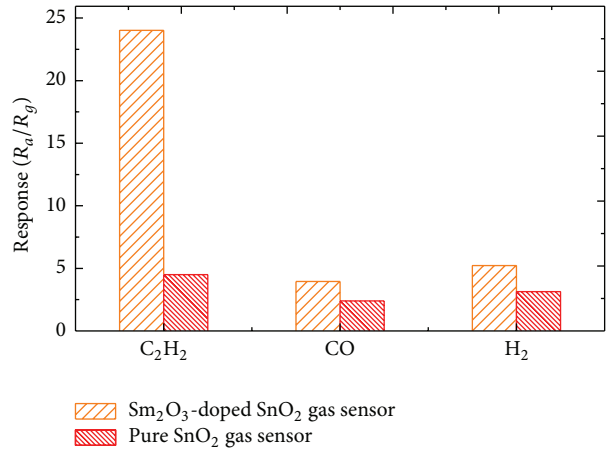

FIGURE 11: Selectivity of the pure and Sm_2O_3 decorated SnO_2 nanorods sensors to 20 μL/L of C_2H_2, CO, and H_2 at 260°C.

the carrier concentration and an increased sensor resistance. As C_2H_2 gas is introduced, the relevant chemical reactions take place between C_2H_2 gas and the ionized oxygen. The trapped electrons are released back to the conduction band of SnO_2 surface, increasing the conductivity of the sensor; thus a decreased resistance is measured.

Based on the sensing experiments demonstrated above, oxide Sm_2O_3 has a significant impact on improving the sensing properties of SnO_2 based gas sensor to C_2H_2. A possible sensing mechanism of the Sm_2O_3 decorated SnO_2 based sensor to C_2H_2 may be explained as follows [37, 38]. Firstly, oxide Sm_2O_3 might work as an effective catalyst, which benefits the effect of active center for C_2H_2 adsorption. Secondly, the incorporation of Sm^{3+} ions might change the electronic movement and the overlap of electron cloud of SnO_2 sensing material, which further strengthens the electronegativity of carbon-hydrogen triple bond of C_2H_2 and makes it easier for hydrogen dissociation to combine with O^{2-}. Therefore, much more electrons have been released in this process so that SnO_2 resistance declines dramatically. Thirdly, the addition

of Sm_2O_3 could restrict the crystallite growth of SnO_2. That is to say, after decorating both the diameter and the length of the synthesized SnO_2 nanorods diminish, which would provide more active sites for oxygen adsorption and channels for gas sensing. Therefore, the Sm_2O_3 decorated SnO_2 based sensor exhibits a higher gas response at a relatively lower operating temperature to C_2H_2 gas with rapid response-recovery, excellent stability, reproducibility, and selectivity.

4. Conclusions

In this work, pure and oxide Sm_2O_3 decorated SnO_2 nanorods were successfully synthesized with a facile and simple hydrothermal method and carefully characterized by XRD, FESEM, TEM, EDS, and XPS measurements, respectively. Planar chemical gas sensors with the synthesis samples were fabricated, and their sensing performances to C_2H_2 gas were systematically performed and automatically recorded by a CGS-1 TP intelligent gas sensing analysis system. Compared with the pure one, the Sm_2O_3 decorated SnO_2 nanorods based sensor exhibits lower optimum operating temperature, higher sensing response, quick response and response time, good stability and reproducibility, and excellent selectivity among potential interface gases. All results indicate the sensor fabricated with oxide Sm_2O_3 decorated SnO_2 nanorods might be a promising candidate for C_2H_2 detection in practice.

Conflict of Interests

The authors declare that there is no conflict of interests regarding the publication of this paper.

Acknowledgments

This work has been supported in part by the National Natural Science Foundation of China (nos. 51507144 and 51277185), Fundamental Research Funds for the Central Universities (nos. XDJK2015B005 and SWU114051), National Special Fund for Major Research Instrumentation Development (no. 2012YQ160007), and the Funds for Innovative Research Groups of China (no. 51021005).

References

[1] Q. Zhou, W. G. Chen, S. D. Peng, and W. Zeng, "Hydrothermal synthesis and acetylene sensing properties of variety low dimensional zinc oxide nanostructures," *The Scientific World Journal*, vol. 2014, Article ID 489170, 8 pages, 2014.

[2] T. Somekawa, M. Kasaoka, F. Kawachi, Y. Nagano, M. Fujita, and Y. Izawa, "Analysis of dissolved C_2H_2 in transformer oils using laser Raman spectroscopy," *Optics Letters*, vol. 38, no. 7, pp. 1086–1088, 2013.

[3] D. R. Morais and J. G. Rolim, "A hybrid tool for detection of incipient faults in transformers based on the dissolved gas analysis of insulating oil," *IEEE Transactions on Power Delivery*, vol. 21, no. 2, pp. 673–680, 2006.

[4] C. M. Quintella, M. Meira, W. L. Silva et al., "Development of a spectrofluorimetry-based device for determining the acetylene content in the oils of power transformers," *Talanta*, vol. 117, no. 15, pp. 263–267, 2013.

[5] A. Akbari, A. Setayeshmehr, H. Borsi, E. Gockenbach, and I. Fofana, "Intelligent agent-based system using dissolved gas analysis to detect incipient faults in power transformers," *IEEE Electrical Insulation Magazine*, vol. 26, no. 6, pp. 27–40, 2010.

[6] S. Singh and M. Bandyopadhyay, "Dissolved gas analysis technique for incipient fault diagnosis in power transformers: a bibliographic survey," *IEEE Electrical Insulation Magazine*, vol. 26, no. 6, pp. 41–46, 2010.

[7] X. C. Wang, M. G. Zhao, F. Liu, J. F. Jia, X. J. Li, and L. L. Cao, "C_2H_2 gas sensor based on Ni-doped ZnO electrospun nanofibers," *Ceramics International*, vol. 39, no. 3, pp. 2883–2887, 2013.

[8] W. G. Chen, Q. Zhou, T. Y. Gao, X. P. Su, and F. Wan, "Pd-doped SnO_2-based sensor detecting characteristic fault hydrocarbon gases in transformer oil," *Journal of Nanomaterials*, vol. 2013, Article ID 127345, 9 pages, 2013.

[9] X. X. Zhang, J. B. Zhang, R. H. Li, and Y. F. Liao, "Application of hydroxylated single-walled carbon nanotubes for the detection of C_2H_2 gases in transformer oil," *Journal of Computational and Theoretical Nanoscience*, vol. 10, no. 2, pp. 399–404, 2013.

[10] Z. Y. Wu, Y. H. Gong, and Q. X. Yu, "Photoacoustic spectroscopy detection and extraction of discharge feature gases in transformer oil based on 1.5 μ tunable fiber laser," *Infrared Physics & Technology*, vol. 58, no. 5, pp. 86–90, 2013.

[11] W. G. Chen, C. Pan, Y. X. Yun, and Y. Liu, "Wavelet networks in power transformers diagnosis using dissolved gas analysis," *IEEE Transactions on Power Delivery*, vol. 24, no. 1, pp. 187–194, 2009.

[12] J. Zhang, S. Wang, M. Xu et al., "Hierarchically porous ZnO architectures for gas sensor application," *Crystal Growth and Design*, vol. 9, no. 8, pp. 3532–3537, 2009.

[13] J. Gong, Y. Li, Z. Hu, Z. Zhou, and Y. Deng, "Ultrasensitive NH_3 gas sensor from polyaniline nanograin enchased TiO_2 fibers," *Journal of Physical Chemistry C*, vol. 114, no. 21, pp. 9970–9974, 2010.

[14] D. Liu, T. Liu, H. Zhang, C. Lv, W. Zeng, and J. Zhang, "Gas sensing mechanism and properties of Ce-doped SnO_2 sensors for volatile organic compounds," *Materials Science in Semiconductor Processing*, vol. 15, no. 4, pp. 438–444, 2012.

[15] K. J. Choi and H. W. Jang, "One-dimensional oxide nanostructures as gas-sensing materials: review and issues," *Sensors*, vol. 10, no. 4, pp. 4083–4099, 2010.

[16] Y. J. Chen, X. Y. Xue, Y. G. Wang, and T. H. Wang, "Synthesis and ethanol sensing characteristics of single crystalline SnO_2 nanorods," *Applied Physics Letters*, vol. 87, no. 23, Article ID 233503, 3 pages, 2005.

[17] C. Wang, L. Yin, L. Zhang, D. Xiang, and R. Gao, "Metal oxide gas sensors: sensitivity and influencing factors," *Sensors*, vol. 10, no. 3, pp. 2088–2106, 2010.

[18] W. Chen, Q. Zhou, L. Xu, F. Wan, S. Peng, and W. Zeng, "Improved methane sensing properties of Co-doped SnO_2 electrospun nanofibers," *Journal of Nanomaterials*, vol. 2013, Article ID 173232, 9 pages, 2013.

[19] W. Zeng, B. Miao, Q. Zhou, and L. Y. Lin, "Hydrothermal synthesis and gas sensing properties of variety low dimensional nanostructures of SnO_2," *Physica E*, vol. 47, no. 3, pp. 116–121, 2013.

[20] Y.-X. Yin, L.-Y. Jiang, L.-J. Wan, C.-J. Li, and Y.-G. Guo, "Polyethylene glycol-directed SnO_2 nanowires for enhanced

gas-sensing properties," *Nanoscale*, vol. 3, no. 4, pp. 1802–1806, 2011.

[21] B. Wang, L. F. Zhu, Y. H. Yang, N. S. Xu, and G. W. Yang, "Fabrication of a SnO_2 nanowire gas sensor and sensor performance for hydrogen," *Journal of Physical Chemistry C*, vol. 112, no. 17, pp. 6643–6647, 2008.

[22] W. Zeng, T. M. Liu, Z. C. Wang, S. Tsukimoto, M. Saito, and Y. Ikuhara, "Selective detection of formaldehyde gas using a Cd-doped TiO_2-SnO_2 sensor," *Sensors*, vol. 9, no. 11, pp. 9029–9038, 2009.

[23] X. Liu, J. Zhang, X. Guo, S. Wu, and S. Wang, "Enhanced sensor response of Ni-doped SnO_2 hollow spheres," *Sensors and Actuators B: Chemical*, vol. 152, no. 2, pp. 162–167, 2011.

[24] Z. Li and Y. Dzenis, "Highly efficient rapid ethanol sensing based on Co-doped In_2O_3 nanowires," *Talanta*, vol. 85, no. 1, pp. 82–85, 2011.

[25] W. Zeng, T. M. Liu, and Z. C. Wang, "Enhanced gas sensing properties by SnO_2 nanosphere functionalized TiO_2 nanobelts," *Journal of Materials Chemistry*, vol. 22, no. 8, pp. 3544–3548, 2012.

[26] X. Song, Z. Wang, Y. Liu, C. Wang, and L. Li, "A highly sensitive ethanol sensor based on mesoporous ZnO-SnO_2 nanofibers," *Nanotechnology*, vol. 20, no. 7, Article ID 075501, 2009.

[27] X. Zhu, H. Shi, J. Yin et al., "Facile preparation of CuO@SnO_2 nanobelts as a high-capacity and long-life anode for lithium-ion batteries," *RSC Advances*, vol. 4, no. 65, pp. 34417–34420, 2014.

[28] G. Neri, A. Bonavita, G. Micali et al., "Effect of the chemical composition on the sensing properties of In_2O_3-SnO_2 nanoparticles synthesized by a non-aqueous method," *Sensors and Actuators B: Chemical*, vol. 130, no. 1, pp. 222–230, 2008.

[29] F. Pourfayaz, A. Khodadadi, Y. Mortazavi, and S. S. Mohajerzadeh, "CeO_2 doped SnO_2 sensor selective to ethanol in presence of CO, LPG and CH_4," *Sensors and Actuators, B: Chemical*, vol. 108, no. 1-2, pp. 172–176, 2005.

[30] W. G. Chen, Q. Zhou, X. P. Su, L. N. Xu, and S. D. Peng, "Morphology control of tin oxide nanostructures and sensing performances for acetylene detection," *Sensors & Transducers*, vol. 154, no. 7, pp. 195–200, 2013.

[31] Z. H. Jing and J. H. Zhan, "Fabrication and gas-sensing properties of porous ZnO nanoplates," *Advanced Materials*, vol. 20, no. 23, pp. 4547–4551, 2008.

[32] W. Zeng, T. M. Liu, D. J. Liu, and E. J. Han, "Hydrogen sensing and mechanism of M-doped SnO_2 (M=Cr^{3+}, Cu^{2+} and Pd^{2+}) nanocomposite," *Sensors and Actuators B: Chemical*, vol. 160, no. 1, pp. 455–462, 2011.

[33] H. Huang, C. K. Lim, M. S. Tse, J. Guo, and O. K. Tan, "SnO_2 nanorod arrays: low temperature growth, surface modification and field emission properties," *Nanoscale*, vol. 4, no. 5, pp. 1491–1496, 2012.

[34] X. F. Liu, J. Iqbal, S. L. Yang, B. He, and R. H. Yu, "Nitrogen doping-mediated room-temperature ferromagnetism in insulating Co-doped SnO_2 films," *Applied Surface Science*, vol. 256, no. 14, pp. 4488–4492, 2010.

[35] Q. Qi, T. Zhang, L. Liu, and X. Zheng, "Synthesis and toluene sensing properties of SnO_2 nanofibers," *Sensors and Actuators, B: Chemical*, vol. 137, no. 2, pp. 471–475, 2009.

[36] J. Yu, D. Zhao, X. Xu, X. Wang, and N. Zhang, "Study on RuO_2/SnO_2: novel and active catalysts for CO and CH_4 oxidation," *ChemCatChem*, vol. 4, no. 8, pp. 1122–1132, 2012.

[37] Q. Qi, T. Zhang, X. J. Zheng et al., "Electrical response of Sm_2O_3-doped SnO_2 to C_2H_2 and effect of humidity interference," *Sensors and Actuators B: Chemical*, vol. 134, no. 1, pp. 36–42, 2008.

[38] S. Ahmadnia-Feyzabad, Y. Mortazavi, A. A. Khodadadi, and S. Hemmati, "Sm_2O_3 doped-SnO_2 nanoparticles, very selective and sensitive to volatile organic compounds," *Sensors and Actuators B: Chemical*, vol. 181, no. 5, pp. 910–918, 2013.